

Dissolution of biogenic silica from land to ocean: Role of salinity and pH

Socratis Loucaides,¹ Philippe Van Cappellen, and Thilo Behrends

Department of Earth Sciences—Geochemistry, Utrecht University, P.O. Box 80.021, 3508 TA Utrecht, the Netherlands

Abstract

The dissolution rates of diatom frustules, phytoliths, two diatomaceous lake sediments, a siliceous ooze from the Southern Ocean, a diatomite deposit, and a synthetic amorphous silica were measured in flow-through reactors supplied with either seawater or freshwater. Although the rates varied by more than one order of magnitude among the different siliceous materials, for any given solid the rate was systematically higher in seawater than freshwater, on average by a factor of five. Flow-through reactor experiments with the diatom frustules and synthetic silica using mixtures of freshwater and seawater indicated that most of the rate increase occurred for seawater fractions between 0 and 50%. The observed rate enhancement is attributed to the higher pH of seawater and the catalytic effect of seawater cations on the hydrolysis of siloxane bonds at the silica surface. Because of their abundance in seawater, Na⁺ and Mg²⁺ are mainly responsible for the salinity-induced rate increase. The large difference in dissolution kinetics between freshwater and seawater helps explain the very efficient recycling of biogenic silica in marine environments compared with freshwater lakes. Enhanced dissolution at the land–ocean transition of biogenic silica produced by terrestrial plants and freshwater diatoms may represent a significant, but largely overlooked, source of nutrient silicon for estuarine and nearshore marine ecosystems.

The production and dissolution of biogenic silica (bSiO₂) in the oceans has been studied extensively, given the importance of diatom primary productivity for the export of organic carbon to the deep sea (Smetacek 2000). However, fixation of silica by land plants, mainly in the form of phytoliths, has been proposed to be of similar magnitude as that by marine diatoms (Conley 2002). Because of the production of bSiO₂ by terrestrial plants, but also by riverine and lacustrine diatoms, much of the reactive Si reaching the oceans has undergone prior biological cycling on the continents. A major fraction of the dissolved Si (dSi) load of the world's rivers may in fact originate from the dissolution of plant litter, soil phytoliths, and freshwater diatom frustules, rather than directly from the chemical weathering of silicate rocks (Derry et al. 2005). In addition, a significant portion of the riverine export of reactive Si may be in the form of bSiO₂ produced on the continents (Conley 1997). Dissolution of this bSiO₂ may constitute an important, but so far largely overlooked, source of nutrient Si for nearshore ecosystems. (Note: reactive Si is defined here as Si that is, or can become, bioavailable on timescales of less than a few years.)

The riverine supply of reactive Si, combined with the availability of light and increased water residence times,

creates favorable conditions for biosiliceous productivity in estuaries and coastal embayments (Lemaire et al. 2002). It has long been suspected that the large increase in salinity at the land–ocean interface promotes diatom production by enhancing the dissolution of bSiO₂ and, thus, the regeneration of bioavailable dSi (Anderson 1986). Nonetheless, to the authors' knowledge, there have been no systematic studies of the role of salinity in the dissolution kinetics of bSiO₂ under Earth surface conditions. Here, we present dissolution rates of a variety of biosiliceous materials measured under ambient conditions in freshwater and seawater, as well as mixtures of both end-member solutions. The goal is to assess to what degree differences in aqueous electrolyte composition may contribute to differences in the recycling efficiency of bSiO₂ in continental, estuarine, and marine environments.

Materials and methods

Biosiliceous materials—Dissolution experiments were carried out with a range of continental and marine biosiliceous materials (Table 1). They include frustules of cultured marine diatoms, phytoliths, siliceous lake sediments, a siliceous ooze from the Southern Ocean, and a diatomite ore deposit. The nonsiliceous fractions of the natural samples were removed as much as possible with the treatments described below. Afterward the samples were rinsed several times with deionized water and freeze dried prior to being used in the dissolution experiments.

The fresh diatoms (*Thalassiosira punctigera*) were cultured at the Royal Netherlands Institute for Sea Research (NIOZ) in central North Atlantic seawater containing low nutrient and trace metal levels. After harvesting the cells, organic matter was removed by low-temperature ashing. Descriptions of the culturing conditions and ashing protocol are given in Koning et al. (2007). Phytoliths were extracted from grass horsetail (*Equisetum*

¹ Corresponding author (s.loucaides@geo.uu.nl).

Acknowledgments

We thank Erica Koning (Netherlands Institute for Sea Research [NIOZ]) for providing the cultures of *T. punctigera*, the *E. rex* ooze sample, and the seawater used in our experiments. We also thank the Celite Corporation for providing us with the diatomite ore sample. The phytolith sample was kindly provided by Loredana Saccone. The diatomaceous sediments from Lake Myvatn and Lake Pavin were collected by former student Laurent Voitel. The comments and suggestions of two journal reviewers significantly improved the manuscript. Financial support for this project was partly provided by the EU-funded Research Training Network SiWEBS (contract number HPRN-CT-2002-000218).

Table 1. Siliceous materials used in the dissolution experiments.

ID	Material	Origin/description	Composition*	Further information
TP	Fresh diatom frustules	Monoculture of marine diatom <i>Thalassiosira punctigera</i> grown in open ocean surface water	Very low impurity levels, Al/Si=0.001	Dissolution kinetics (Van Cappellen et al. 2002b); ultrastructure (Vrieling et al. 2000)
EQ	Fresh phytoliths	Oxidative extraction of whole plant horsetails (<i>Equisetum arvense</i>)	Very low impurity levels, Al/Si<0.001	Morphology, surface chemistry, and dissolution kinetics (Frayse et al. 2006)
LP	Biosiliceous lake sediment	Lake Pavin upper 2 cm of sediment core collected at 61-m water depth	Al/Si=0.012, Fe/Si=0.003, K/Si=0.002	Geochemical studies/environmental setting (Viollier et al. 1997)
LM	Biosiliceous lake sediment	Lake Myvatn upper 2 cm of sediment core collected at 31-m water depth	Al/Si=0.008, Fe/Si=0.009, K/Si=0.001	Environmental setting/ecology (Einarsson 2004)
ER	<i>E. rex</i> biosiliceous ooze sample	Weddell Sea: sample from 1-m thick diatomaceous layer in core collected at 3,550-m water depth	Al/Si=0.003	Core location, dating, formation, environmental setting (Abelmann et al. 1988); dissolution kinetics (Koning et al. 2007 and references therein)
DI	Diatomite ore	Miocene diatomaceous earth deposit from a mine in Lompoc, California	Al/Si=0.029, Fe/Si=0.007, K/Si=0.005	Paleoenvironment and species composition (Moyle and Dolley 2002)
AE	Aerosil® OX50; synthetic amorphous silica	Fumed silica	Very pure; well-characterized physicochemical properties	www.aerosil.com

* Atomic ratios are based on inductively coupled plasma mass spectrometry (ICP-MS) analyses after total destruction of the samples.

arvense), a known silicon accumulating plant, by means of a chemical oxidation method combining hydrogen peroxide and nitric acid. Plant tissue was boiled in 30% H₂O₂ until the reaction ceased, and then plant tissue was digested in concentrated HNO₃ at 60°C for 1–2 h. Information on the morphology, surface chemical properties, and dissolution kinetics of horsetail phytoliths can be found in Frayse et al. (2006).

Core-top sediments were collected from two shallow lakes, one located in France (Pavin), the other in Iceland (Myvatn). Both lakes experience seasonal diatom blooms, which cause the accumulation of biosiliceous sediments (Viollier et al. 1997; Einarsson 2004). The marine biosiliceous ooze is of Pliocene age; it was obtained from a core from the Weddell Sea, within a layer consisting nearly exclusively of fragments of frustules from the diatom species *Ethmodiscus rex*. Descriptions of the core and the *E. rex* layer sampled are given in Abelmann et al. (1988). The diatomite was obtained as untreated ore material from a commercial mine in Lompoc, California, and dates from the Miocene. Details on the depositional setting and composition of the diatomite are summarized in Moyle and Dolley (2002). The various sediment samples were homogenized and air dried prior to cleaning. Organic matter was removed by low-temperature ashing, which involved placing the samples for 4 h in a Plasmarep 300 plasma oven (~40°C). Subsequently, they were washed in 1 mol L⁻¹ HCl overnight, in order to remove traces of CaCO₃.

A fumed silica (Aerosil® OX50, Degussa GmbH) of high chemical purity was used as a synthetic reference material. Its specific surface area (50 m² g⁻¹) falls within the typical range of diatom frustules and plant phytoliths (Dixit et al.

2001; Frayse et al. 2006). The material was used as received in the experiments.

Flow-through reactors—The application of flow-through reactors to measure dissolution rates of marine and terrestrial biosiliceous materials is described in detail in a number of publications (Van Cappellen et al. 2002a and references therein). Briefly, a known mass of siliceous solid is suspended in a reactor cell through which an undersaturated solution flows at a constant rate controlled by a peristaltic pump. After the dSi concentration in the outflow reaches a constant value, the steady state dissolution rate *R* is calculated according to

$$R = \frac{([dSi]_{out} - [dSi]_{in})q}{M} \quad (1)$$

where [dSi]_{out} and [dSi]_{in} are the dSi concentrations measured in the outflow and inflow solutions, respectively; *q* is the volumetric flow rate through the reactor; and *M* is the mass of siliceous solid material in the reactor. Note that, owing to dissolution, *M* decreases with time, and its value in Eq. 1 was therefore corrected after each sampling to account for the silica mass loss due to dissolution. The total fraction of solid silica dissolved by the end of the experiments varied from 1% for the least reactive materials (DI and ER, Table 1) to 25% for the phytolith sample (EQ).

The flow-through reactors used in this study consisted of a cylindrical Plexiglas® cell with a fixed bottom and a removable top. A floating Teflon-coated magnetic stir bar kept the suspension inside the reactor well mixed, and a 0.2-μm pore-size membrane filter at the outflow prevented the solid material from leaving the reactor. The net volume of

Table 2. Summary of experimental conditions and results of flow-through dissolution experiments. Each listing corresponds to a separate reactor experiment. See Table 1 for the identification of the solids. The pH values are those of the inflow solution. The dissolution rates R were calculated using Eq. 1; standard deviations (SD) are given in parentheses. All experiments were performed at 25°C. FW = freshwater; SW = seawater.

Series	Solid	Input solution	pH	[dSi] _{in} ($\mu\text{mol L}^{-1}$)	[dSi] _{out} ($\mu\text{mol L}^{-1}$)	R (SD) ($\mu\text{mol g}^{-1} \text{h}^{-1}$)	
A	EQ	FW	6.3	120	440	3.2 (0.9)	
	EQ	SW	8.1	2.4	1,699	17 (0.4)	
	LP	FW	6.3	120	260	1.4 (0.2)	
	LP	SW	8.1	2.4	867	8.7 (0.4)	
	LM	FW	6.3	120	361	2.4 (0.2)	
	LM	SW	8.1	2.4	949	9.5 (0.9)	
	ER	FW	6.3	120	130	0.1 (0.03)	
	ER	SW	8.1	2.4	42	0.4 (0.06)	
	DI	FW	6.3	120	143	0.2 (0.02)	
	DI	SW	8.1	2.4	68	0.7 (0.04)	
	B	AE	FW	6.3	120	358	2.4 (0.4)
		AE	1%SW	6.5	117	439	3.2 (0.7)
AE		10%SW	7.4	109	700	5.9 (1.3)	
AE		25%SW	7.6	91	810	7.2 (0.7)	
AE		50%SW	7.7	69	1,081	10.1 (1.3)	
AE		75%SW	7.9	31	1,146	11.2 (1.4)	
AE		SW	8.1	2.4	1,169	11.7 (1.0)	
TP		FW	6.3	120	209	0.9 (0.1)	
TP		1%SW	6.5	117	252	1.3 (0.2)	
TP		10%SW	7.4	109	364	2.5 (0.4)	
TP		25%SW	7.6	91	451	3.6 (0.2)	
TP		50%SW	7.7	69	484	4.1 (0.6)	
TP		75%SW	7.9	31	393	3.6 (0.3)	
TP		SW	8.1	2.4	365	3.7 (0.3)	
C		AE	FW	8.1	120	542	4.2 (0.2)
	TP	FW	8.1	120	298	1.8 (0.2)	
	EQ	FW	8.1	120	740	6.2 (0.5)	
	LM	FW	8.1	120	630	5.1 (0.6)	
D	AE	0.05 mol L ⁻¹ MgCl ₂	6.3	120	521	4.0 (0.3)	
	AE	0.01 mol L ⁻¹ KCl	6.3	120	444	3.2 (0.2)	
	AE	0.41 mol L ⁻¹ NaCl	6.3	120	569	4.5 (0.3)	
	AE	0.01 mol L ⁻¹ CaCl ₂	6.3	120	458	3.4 (0.5)	
	AE	MgCl ₂ I=0.7 mol L ⁻¹	6.3	120	818	7.0 (0.8)	
	AE	KCl I=0.7 mol L ⁻¹	6.3	120	708	5.9 (0.8)	
	AE	NaCl I=0.7 mol L ⁻¹	6.3	120	719	6.0 (0.7)	
	AE	CaCl ₂ I=0.7 mol L ⁻¹	6.3	120	565	4.4 (0.5)	

each reactor (stir bar volume subtracted) was 25 mL. The flow rate in all experiments was adjusted to 1 mL h⁻¹ using a peristaltic pump. The reactors were kept at a constant temperature of 25°C in a water bath placed on top of a 15 position multistirring plate.

The initial solid-to-solution ratio was 4 g L⁻¹ in all flow-through experiments. The outflow of the reactors was sampled every reactor volume (i.e., each 25 h) for periods of 7–10 d. Samples were collected in plastic 15-mL Greiner® centrifuge tubes, and the dissolved silica content was analyzed colorimetrically on a nutrient Bran and Luebbe autoanalyzer (relative standard deviation 0.5%). The pH values of inflow and outflow solutions were measured using a Metrohm Unitrode combined glass pH electrode calibrated daily with commercial buffers.

The dissolution rates reported are averages of the rates calculated with Eq. 1 using the measured outflow concentrations [dSi]_{out} and the corrected solid masses M . Typically, the outflow dSi concentrations stabilized after three to four reactor volumes (i.e., after 75–100 h), and the

average dissolution rates were based on the [dSi]_{out} values measured in the subsequent five to seven reactor volumes of outflow.

Flow-through dissolution experiments—In a first series of flow-through reactor experiments (series A, Table 2), dissolution rates were measured using either filtered (0.45- μm pore size) seawater from the oligotrophic central part of the North Atlantic (dSi \sim 2 $\mu\text{mol L}^{-1}$, pH 8.1) or a very dilute (ionic strength \sim 2 \times 10⁻⁴ mol L⁻¹), slightly acidic (pH 6.3) Ca-Na-HCO₃ commercial mineral water (SPA Bleu®). In addition to the end-member seawater and freshwater solutions, dissolution rates of fresh diatom frustules (TP) and synthetic amorphous silica (AE) were also measured in freshwater–seawater mixtures (series B, Table 2). Five intermediate salinities were created corresponding to solutions of 1%, 10%, 25%, 50%, and 75% seawater. Of the natural biosiliceous materials, only TP was available in large enough quantities to carry out the full set of mixture experiments.

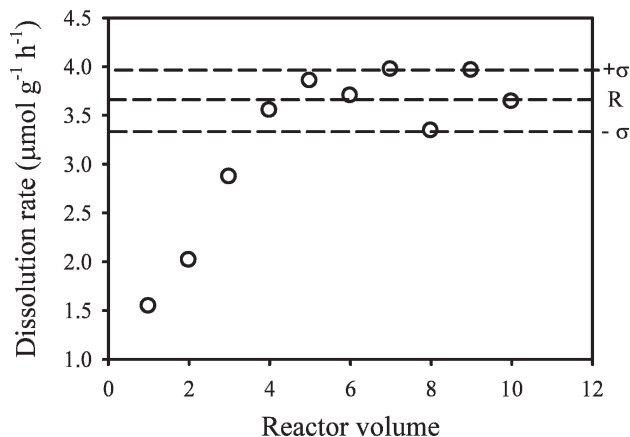


Fig. 1. Dissolution rate of fresh diatom frustules (TP) measured in a flow-through reactor supplied with seawater. The points correspond to rates calculated with Eq. 1, using the measured outflow concentrations of dissolved silica ($[dSi]_{out}$). The rates are plotted against the volume of seawater that has flowed through the reactor, expressed in units of reactor volumes. Steady state outflow $[dSi]_{out}$ concentrations are reached after three reactor volumes of flow. The dissolution rates R reported in Table 2 are the average rate values obtained, after steady state conditions were reached. Standard deviations (σ) of the rates are also reported in Table 2. They mainly reflect the experimental variations in the measured $[dSi]_{out}$ values.

To separate the effects of dissolved salts and pH, further flow-through experiments were carried out with freshwater inflow solutions whose pH was adjusted to that of seawater (8.1) by the addition of 0.01 mol L^{-1} NaOH (series C, Table 2). The addition of base (2.2 mL of 0.01 mol L^{-1} NaOH in 500 mL freshwater) increased the ionic strength of the solution by less than $5 \times 10^{-5} \text{ mol L}^{-1}$. Three of the natural materials were used in these experiments (TP, LM, and EQ). Finally, the effects of the major seawater cations (Na^+ , K^+ , Mg^{+2} , and Ca^{+2}) on the dissolution kinetics of synthetic amorphous silica (AE) were investigated by adding chloride salts (reagent grade NaCl, KCl, MgCl_2 , or CaCl_2) separately to the end-member freshwater (series D, Table 1). Two sets of inflow solutions were prepared: in the first one, the amount of salt was adjusted to reach the average seawater concentration of the corresponding cation, in the second one, salt addition was adjusted to obtain solutions of constant ionic strength, equal to that of seawater ($I = 0.7 \text{ mol L}^{-1}$).

Solubility measurements—The solubilities of the various siliceous materials were measured in 15-mL batch reactors placed in a 25°C water bath. The solid-to-solution ratios were relatively high, 10 g L^{-1} , in order to reduce the time required to reach solubility equilibrium. The solids were suspended in 0.1 mol L^{-1} NaCl solutions made up of deionized water and reagent grade NaCl to which Tris-base buffer was added in order to maintain pH at 8.0 ± 0.2 . The dissolved silica concentration was monitored periodically; the value at which it stabilized was considered the apparent silica solubility of the corresponding material. An additional series of batch experiments with the fresh diatom frustules (TP) was carried out in freshwater–seawater

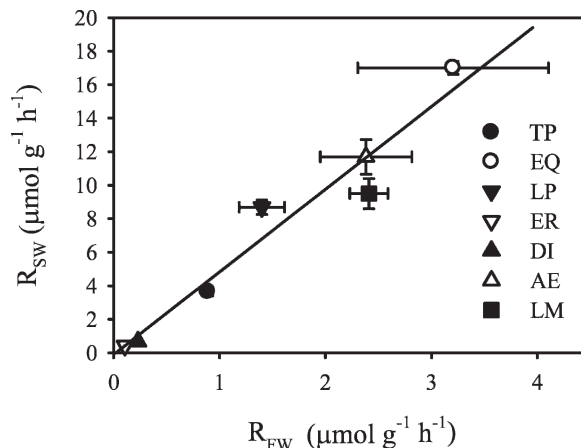


Fig. 2. Dissolution rates in seawater vs. dissolution rates in freshwater at 25°C of all siliceous materials (Table 1). The strong linear relationship ($r^2 = 0.95$) indicates an average fivefold rate increase in seawater vs. freshwater. The error bars represent standard deviations of the rate determinations (see Fig. 1).

mixtures identical to those of series B (Table 2). These experiments were designed to determine whether the apparent solubility of biogenic silica depends on the solution composition.

Results

Dissolution rates reached steady state after three to four reactor volumes of flow (Fig. 1). Standard deviations on the average steady state rates were on the order of 10–15%. These standard deviations are reported in Table 2 and represented by error bars in the figures where appropriate. The measured dissolution rates varied over more than two orders of magnitude (Table 2). As shown by the results for series A and B, a significant part of this variability could be ascribed to the nature of the inflow solution. For any given siliceous material, the rate was systematically higher in seawater than in freshwater (Fig. 2): rates increased on average by a factor of five between freshwater and seawater.

Not unexpectedly, the slowest rates were observed for the oldest materials (ER and DI). These materials also experienced somewhat lower increases in rate between freshwater and seawater (3.8 times higher for ER and 2.9 for DI). The highest rates were obtained for the fresh phytoliths (EQ) and synthetic amorphous silica (AE). Intermediate rates were observed for the core-top lake sediments (LP and LM) and fresh diatom frustules (TP).

The rates measured for TP and AE in freshwater–seawater mixtures (series B, Table 2) progressively increased with increasing seawater addition, leveling off beyond a 1:1 mixing ratio (Fig. 3). The largest relative increases in dissolution rates were observed between pure freshwater and the 10% seawater mixture. The rates measured in pH 8.1 freshwater were higher than those in pH 6.3 freshwater (series C, Table 2). For the four materials used (EQ, TP, LM, and AE), on the order of $44 \pm 9\%$ of the rate increase between freshwater and seawater could be attributed to the change in pH from 6.3

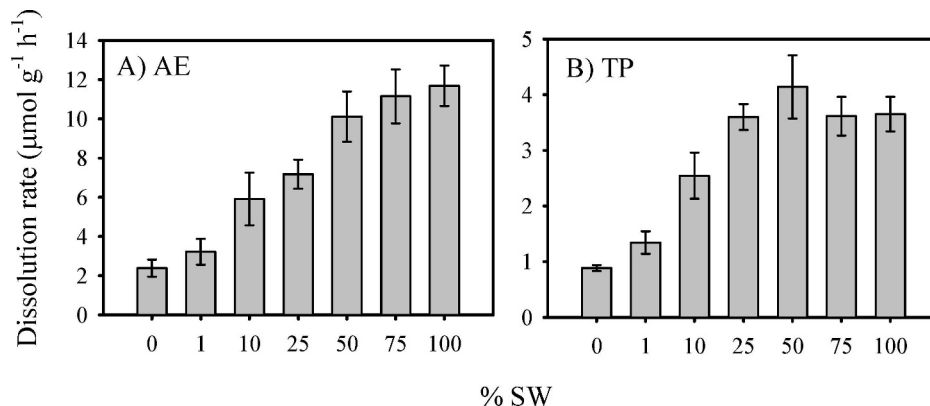


Fig. 3. (A) Dissolution rates R of Aerosil® OX50 (AE) and (B) fresh diatom frustules (TP) at 25°C in freshwater–seawater mixtures. The x -axis indicates the percentage of seawater (SW) in the mixtures. The error bars represent standard deviations of the rate determinations (see Fig. 1).

to 8.1, with the remaining increase representing the effect of the dissolved seawater salts on the dissolution kinetics (Fig. 4).

The salt-amended freshwater experiments (series D, Table 2) clearly showed the rate-enhancing effects of dissolved cations (Fig. 5). Together the individual effects of the two major seawater cations, Na^+ and Mg^{+2} , could largely account for the salt-induced increase in dissolution rate of AE between freshwater and seawater (i.e., after accounting for the pH difference). At constant seawater ionic strength, the rate enhancements of Mg^{+2} , Na^+ , and K^+ were comparable within errors, while Ca^{+2} had a distinct lesser effect (Fig. 6).

The dSi buildup in the ($0.1 \text{ mol L}^{-1} \text{ NaCl}$) batch solubility experiments with fresh biosiliceous materials (EQ and TP), core-top lake sediments (LP and LM), and synthetic amorphous silica (AE) stabilized after 1–4 weeks of equilibration time. For the diatomite (DI), apparent solubility equilibrium was reached after 24 weeks, while for

the *E. rex* ooze (ER) continued increase in dSi was observed for a period exceeding 2 yr. The solubility value reported for ER in Table 3 corresponds to the dSi concentration measured after 107 weeks. For both end-member solutions (freshwater and seawater), the observed dissolution rates of the different materials correlated positively with the apparent silica solubilities (Fig. 7). The batch experiments with TP in freshwater–seawater mixtures showed no significant variation of the solubility with solution composition (<10%, results not shown).

Discussion

Salt and pH effects on silica dissolution kinetics—Both increased salt concentration and increased pH contribute to the rate enhancement of bSiO_2 in seawater relative to freshwater (Fig. 4). The observed solution effects on the dissolution kinetics can be understood in terms of the chemical structure and reactivity of the silica–water interface (Dove 1999; Van Cappellen et al. 2002a).

There is general agreement that dissolution of SiO_2 at near-neutral pH is due to nucleophilic attack of water molecules that cause the breaking of siloxane bonds, $>\text{Si}-\text{O}-\text{Si}<$, at the particle surface (Dove and Crerar 1990). As a water molecule approaches a surface silicon atom, the transfer of electron density weakens the adjacent siloxane Si–O bond, which eventually breaks. The now open linkages bind with the dissociating water molecule to form $>\text{Si}-\text{OH}$ (silanol) groups. The process is then repeated until all siloxane bonds surrounding the surface silicon are broken, and the latter leaves the surface in the form of a silicic acid molecule, $\text{Si}(\text{OH})_4$.

Increasing pH leads to the deprotonation of surface silanol groups, thereby further facilitating the breaking of the bridging siloxane bonds (Dove and Elston 1992). Base-promoted dissolution occurs when the solution pH exceeds the point of zero surface charge (pH_{zpc}) of the solid, which for bSiO_2 falls in the range 1.2–4 (Dixit and Van Cappellen 2002; Fraysse et al. 2006). The catalyzing effect of increased pH, for $\text{pH} > \text{pH}_{\text{zpc}}$, has been demonstrated previously for marine diatomaceous silica (Van Cappellen and Qiu 1997) and plant phytoliths (Fraysse et al. 2006).

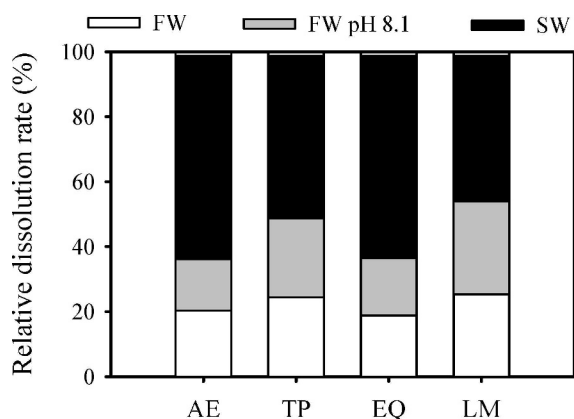


Fig. 4. Dissolution rates of the synthetic silica (AE), fresh diatom frustules (TP), phytoliths (EQ), and Lake Myvatn sediments (LM) measured in freshwater and in freshwater with pH adjusted to that of seawater (pH 8.1), relative to the dissolution rates in seawater. The gray and black bars indicate the relative contributions to the rate enhancement in seawater of pH and dissolved salts, respectively. All rate measurements were done at 25°C.

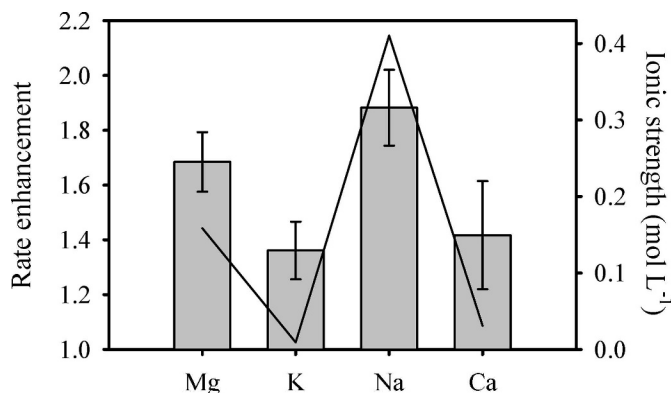


Fig. 5. Dissolution rate enhancements by individual seawater cations at 25°C and pH 6.3. The cations were added as chloride salts to the freshwater to match their respective concentrations in seawater. The bars represent the rate enhancement in the cation-amended solution, relative to the rate in freshwater, and the line indicates the ionic strengths of the cation-amended solutions. The error bars represent standard deviations of the rate determinations (see Fig. 1).

Enhanced dissolution rates of quartz in salt solutions are well documented (Dove 1999 and references therein). Dove (1999) proposes that the cations of alkali metals and alkaline earth elements strengthen the nucleophilic properties of water molecules at the quartz surface. Hydrated cations adsorbed to the negatively charged SiO₂ surface improve the physical access of water to siloxane bonds by redirecting hydration waters into more favorable positions, thereby increasing the rate of hydrolysis of the bonds. It should be noted, however, that the exact molecular mechanism whereby aqueous cations catalyze silica dissolution is not yet fully elucidated.

Dove and Crerar (1990) showed that the dependence of the dissolution rate of quartz on the concentrations of individual alkali and alkaline earth cations follows Langmuir-type isotherms, where the rate initially increases sharply upon addition of the cation and then asymptotically approaches a maximum value with continued increase in cation concentration. This behavior is in line with the freshwater–seawater mixture experiments, where the dissolution rates level off for the highest admixtures of seawater (Fig. 3). The results shown in Fig. 5 also indicate that the rate-enhancing effects of Na⁺, K⁺, Mg²⁺, and Ca²⁺ depend nonlinearly on the cation concentrations. While Na⁺ and Mg²⁺ are the main rate-enhancing cations in seawater by virtue of their abundance, Ca²⁺ and K⁺ have nonetheless significant catalytic effects despite their much lower concentrations.

Solutions of MgCl₂, NaCl, and KCl appear more effective in enhancing the rate of synthetic amorphous silica than CaCl₂ (Fig. 6). In contrast, for quartz, Dove and Nix (1997) found that the dissolution rate enhancement in single cation solutions increases in the order Mg²⁺ < Ca²⁺ ≈ Li⁺ ≈ Na⁺ ≈ K⁺ < Ba²⁺ at 200°C and near-neutral pH, while House (1994) reports higher quartz dissolution rates in CaCl₂ than in NaCl solution at 25°C and pH 10. Thus, further studies in single and multiple salt solutions are needed to systematically delineate the effects of ionic

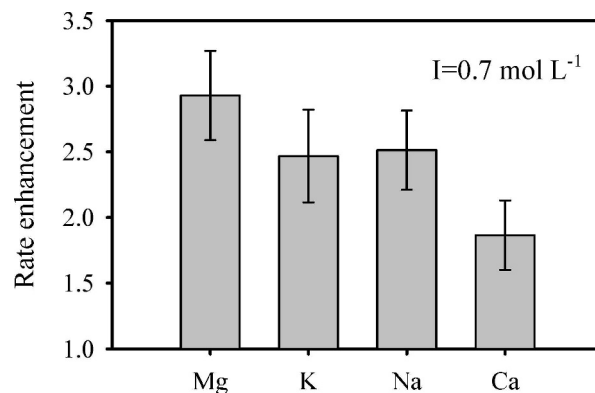


Fig. 6. Dissolution rate enhancement by individual seawater cations at 25°C and pH 6.3. The cations were added as chloride salts to freshwater to a constant ionic strength of 0.7 mol L⁻¹. The error bars represent standard deviations of the rate determinations (see Fig. 1).

constituents on the dissolution of bSiO₂ under Earth surface conditions. Preliminary results, for instance, indicate that the rate enhancement of amorphous silica at 25°C and near-neutral pH may be less in Na₂SO₄ than in NaCl solution (results not shown).

Solubility and reactivity of biogenic silicas—All the siliceous materials used in this study exhibit significant rate enhancement in seawater relative to freshwater, although the absolute dissolution rates vary over more than one order of magnitude (Fig. 7). The rates correlate positively with the apparent silica solubilities, in agreement with the linear free energy relationship (LFER) for silica dissolution proposed by Wollast (1974), which includes crystalline as well as amorphous forms of SiO₂.

The pure synthetic amorphous silica (AE) exhibits the highest solubility of all the samples used (1,960 μmol L⁻¹). The solubilities of the phytoliths, fresh diatom frustules, and core-top lake sediments (1,750–1,950 μmol L⁻¹), however, are very close to that of AE and similar to 25°C

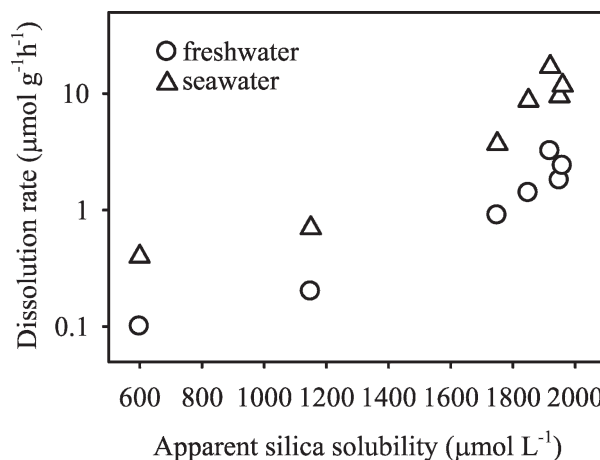


Fig. 7. Dissolution rates of all the biogenic and synthetic siliceous materials measured at 25°C in freshwater and seawater, plotted against the apparent silica solubility measured in 0.1 mol L⁻¹ NaCl, at pH 8 and 25°C.

Table 3. Apparent silica solubilities of the various siliceous materials in 0.1 mol L⁻¹ NaCl, at pH 8.0 and 25°C (see Table 1 for identification of the solids). The value reported for the *E. rex* ooze is a minimum estimate, since the concentration of dissolved silica was still slowly increasing after 107 weeks of incubation.

Solid	[dSi] _{eq} (μmol L ⁻¹)
TP	1,750
EQ	1,920
LP	1,850
LM	1,950
ER	600
DI	1,150
AE	1,960

solubility values for fresh diatoms reported in the literature (Dixit et al. 2001 and references therein). The significantly lower solubilities of the diatomite (DI) and *E. rex* ooze (ER) fall in between the apparent silica solubilities measured on Southern Ocean core-top siliceous oozes (Van Cappellen and Qiu 1997) and the lowest values reported for fossil diatoms (~200 μmol L⁻¹, Hurd and Theyer 1974). The concomitant drop in solubility and reactivity of fossil biogenic silicas relative to fresh bSiO₂ reflects alterations of the bulk structure and surface chemistry. For diatom frustules, these changes may start during sedimentation through the water column (Rickert et al. 2002) and continue after burial in sediments (Van Cappellen et al. 2002a,b). Processes that may decrease the solubility and reactivity of bSiO₂ include the incorporation of impurities, such as aluminum (Van Cappellen et al. 2002b), the lowering of the specific surface area (Van Cappellen et al. 2002b), and the progressive condensation of the silica framework (Gendron-Badou et al. 2003).

Implications—The regeneration of dSi from bSiO₂ depends on a variety of environmental conditions, processes, and material properties (for a review, see Van Cappellen et al. 2002a). An important first step is the removal of protective organic coatings covering the silica surfaces, typically through bacterial activity (Bidle and Azam 1999). Once exposed, the silica surfaces dissolve because most natural waters are undersaturated with respect to bSiO₂. In addition to the degree of undersaturation, the dissolution rate of a given biosiliceous material depends on the temperature, pH, and, as shown here, the ionic composition of the aqueous medium.

The large, fivefold, enhancement of the dissolution rate of bSiO₂ observed in seawater relative to freshwater implies that changes in salinity and pH should significantly modify the biogeochemical cycling of nutrient silicon across the land to ocean transition. In particular, it helps explain differences in recycling efficiency of silica in marine and freshwater ecosystems. Recycling of bSiO₂ in the oceans is extremely efficient, with globally only about 5–7% of the diatomaceous bSiO₂ exported from the euphotic zone ultimately being buried in sediments (Tréguer et al. 1995). In comparison, recent mass balance estimates for Lake Baikal, one of the world's largest (31,500 km²) and deepest

(1,637 m maximum water depth) freshwater lakes, indicate that more than 50% of the bSiO₂ export production is buried in the sediments (Muller et al. 2005). While a variety of factors may contribute to the high preservation potential of bSiO₂ in Lake Baikal, the low salinity (<0.1) and near-neutral pH (7.1–7.2) (Falkner et al. 1997) are likely to play an important role.

A significant fraction of reactive Si is exported from the continents as phytoliths or diatom frustules (Conley 1997). Survival of bSiO₂ during river transport is consistent with its relatively slow dissolution kinetics in continental freshwaters. For example, the dissolution rate of *T. punctigera* measured in the freshwater end-member corresponds to a half-life of the frustules of 1.3 yr. Siliceous productivity in estuaries and marginal environments further increases the proportion of reactive Si that reaches the oceans in the form bSiO₂. According to a recent reassessment of the biogeochemical Si cycle, bSiO₂ could represent up to 40% of the reactive Si input to the distal coastal ocean (Laruelle unpubl.).

The large influx of bSiO₂, together with the salinity-dependent dissolution kinetics, creates favorable conditions for intense regeneration of nutrient silicon at the confluence of continental and marine waters. A recent comparison of Si cycling in intertidal marshes suggests that salinity may be a determining factor responsible for faster bSiO₂ recycling in salt marshes of the Scheldt estuary, compared with upstream, freshwater marshes (Struyf et al. 2006). Other workers have also proposed that salinity increase may in part be responsible for the high regeneration of dSi in the mid-salinity regions of estuaries (Anderson 1986).

While the results of this study clearly show that the alkaline and saline nature of seawater greatly enhances the oceanic recycling of bSiO₂, they also emphasize the need to better understand the fate of bSiO₂ produced on the continents. The latter is crucial in view of the large changes in nutrient fluxes induced by human activity. In particular, sediment retention by damming and river diversion has a major impact on the riverine export of bSiO₂, which may further exacerbate the proliferation of nonsiliceous phytoplankton in coastal marine environments (Humborg et al. 2000).

References

- ABELMANN, A., R. GERSONDE, AND V. SPIESS. 1988. Pliocene–Pleistocene paleoceanography in the Weddell Sea—Siliceous microfossil evidence, p. 729–759. In U. Bleil and J. Thiede [eds.], Geological history of the polar oceans: Arctic versus Antarctic. NATO Advanced Study Institute Series, Kluwer.
- ANDERSON, G. F. 1986. Silica, diatoms and a freshwater productivity maximum in Atlantic coastal plain estuaries, Chesapeake Bay. *Estuar. Coast. Shelf Sci.* **22**: 183–197.
- BIDLE, K. D., AND F. AZAM. 1999. Accelerated dissolution of diatom silica by marine bacterial assemblages. *Nature* **397**: 508–512.
- CONLEY, D. J. 1997. Riverine contribution of biogenic silica to the oceanic silica budget. *Limnol. Oceanogr.* **42**: 774–777.
- . 2002. Terrestrial ecosystems and the global biogeochemical silica cycle. *Glob. Biogeochem. Cycles* **16**: 1121, doi:10.1029/2002GB001894.

- DERRY, L. A., A. C. KURTZ, K. ZIEGLER, AND O. A. CHADWICK. 2005. Biological control of terrestrial silica cycling and export fluxes to watersheds. *Nature* **433**: 728–731.
- DIXIT, S., AND P. VAN CAPPELLEN. 2002. Surface chemistry and reactivity of biogenic silica. *Geochim. Cosmochim. Acta* **66**: 2559–2568.
- , ———, AND A. J. VAN BENNEKOM. 2001. Processes controlling solubility of biogenic silica and pore water build-up of silicic acid in marine sediments. *Mar. Chem.* **73**: 333–352.
- DOVE, P. M. 1999. The dissolution kinetics of quartz in aqueous mixed cation solutions. *Geochim. Cosmochim. Acta* **63**: 3715–3727.
- , AND D. A. CRERAR. 1990. Kinetics of quartz dissolution in electrolyte solutions using a hydrothermal mixed flow reactor. *Geochim. Cosmochim. Acta* **54**: 955–969.
- , AND S. F. ELSTON. 1992. Dissolution kinetics of quartz in sodium-chloride solutions—analysis of existing data and a rate model for 25°C. *Geochim. Cosmochim. Acta* **56**: 4147–4156.
- , AND C. J. NIX. 1997. The influence of the alkaline earth cations, magnesium, calcium, and barium on the dissolution kinetics of quartz. *Geochim. Cosmochim. Acta* **61**: 3329–3340.
- EINARSSON, Á. 2004. Lake Myvatn and the River Laxá: An introduction. *Aquat. Ecol.* **38**: 111–114.
- FALKNER, K. K., AND OTHERS. 1997. Minor and trace element chemistry of Lake Baikal, its tributaries, and surrounding hot springs. *Limnol. Oceanogr.* **42**: 329–345.
- FRAYSSE, F., O. S. POKROVSKY, J. SCHOTT, AND J.-D. MEUNIER. 2006. Surface properties, solubility and dissolution kinetics of bamboo phytoliths. *Geochim. Cosmochim. Acta* **70**: 1939–1951.
- GENDRON-BADOU, A., T. CORADIN, J. MAQUET, F. FROHLICH, AND J. LIVAGE. 2003. Spectroscopic characterization of biogenic silica. *J. Non-Cryst. Solids* **316**: 331–337.
- HOUSE, W. A. 1994. The role of surface complexation in the dissolution kinetics of silica: Effects of monovalent and divalent ions at 25°C. *J. Colloid Interface Sci.* **163**: 379–390.
- HUMBORG, C., D. CONLEY, L. RAHM, F. WULFF, A. COCIASU, AND V. ITTEKKOT. 2000. Silicon retention in river basins: Far-reaching effects on biogeochemistry and aquatic food webs in coastal marine environments. *Ambio* **29**: 45–50.
- HURD, D. C., AND F. THEYER. 1974. Changes in physical and chemical properties of biogenic silica from the Central Equatorial Pacific. I. Solubility, specific surface area, and solution rate constants of acid-cleaned samples, p. 211–230. *In* T. R. P. J. Gibb [ed.], *Analytical methods in oceanography*. Advances in Chemistry Series. American Chemical Society.
- KONING, E., M. GEHLEN, A. M. FLANK, G. CALAS, AND E. EPPING. 2007. Rapid post-mortem incorporation of aluminum in diatom frustules: Evidence from chemical and structural analyses. *Mar. Chem.* **103**: 97–111.
- LEMAIRE, E., G. ABRIL, R. DE WIT, AND H. ETCHEBER. 2002. Distribution of phytoplankton pigments in nine European estuaries and implications for an estuarine typology. *Biogeochemistry* **59**: 5–23.
- MOYLE, P. R., AND T. P. DOLLEY. 2002. With or without salt: A comparison of marine and continental-lacustrine diatomite deposits. Technical Report. United States Geological Survey. 2209.
- MULLER, B., M. MAERKI, M. SCHMID, E. G. VOLOGINA, B. WEHRLI, A. WUEST, AND M. STURM. 2005. Internal carbon and nutrient cycling in Lake Baikal: Sedimentation, upwelling, and early diagenesis. *Glob. Planet. Change* **46**: 101–124.
- RICKERT, D., M. SCHLUTER, AND K. WALLMANN. 2002. Dissolution kinetics of biogenic silica from the water column to the sediments. *Geochim. Cosmochim. Acta* **66**: 439–455.
- SMETACEK, V. 2000. Oceanography: The giant diatom dump. *Nature* **406**: 574–575.
- STRUYF, E., A. DAUSSE, S. VAN DAMME, K. BAL, B. GRIBSHOLT, H. T. S. BOSCHKER, J. J. MIDDELBURG, AND P. MEIRE. 2006. Tidal marshes and biogenic silica recycling at the land–sea interface. *Limnol. Oceanogr.* **51**: 838–846.
- TRÉGUER, P., D. M. NELSON, A. J. VANBENNEKOM, D. J. DEMASTER, A. LEYNAERT, AND B. QUEGUINER. 1995. The silica balance in the world ocean—a reestimate. *Science* **268**: 375–379.
- VAN CAPPELLEN, P., S. DIXIT, AND M. GALLINARI. 2002a. Biogenic silica dissolution and the marine Si cycle: Kinetics, surface chemistry and preservation. *Oceanis* **28**: 417–454.
- , ———, AND J. VAN BEUSEKOM. 2002b. Biogenic silica dissolution in the oceans: Reconciling experimental and field-based dissolution rates. *Glob. Biogeochem. Cycles* **16**: 1075, doi:10.1029/2001GB001431.
- , AND L. QIU. 1997. Biogenic silica dissolution in sediments of the Southern Ocean. II. Kinetics. *Deep-Sea Res. II* **44**: 1129–1149.
- VIOLLIER, E., G. MICHARD, D. JEZEQUEL, M. PEPE, AND G. SARAZIN. 1997. Geochemical study of a crater lake: Lake Pavin, Puy de Dome, France. Constraints afforded by the particulate matter distribution in the element cycling within the lake. *Chem. Geol.* **142**: 225–241.
- VRIELING, E. G., T. P. M. BEELEN, R. A. VAN SANTEN, AND W. W. C. GIESKES. 2000. Nanoscale uniformity of pore architecture in diatomaceous silica: A combined small and wide angle X-ray scattering study. *J. Phycol.* **36**: 146–159.
- WOLLAST, R. 1974. The silica problem, p. 359–392. *In* E. D. Goldberg [ed.], *The sea*. Wiley Interscience.

Received: 26 September 2007

Accepted: 12 February 2008

Amended: 9 March 2008